Atmos. Chem. Phys., 17, 2759–2774, 2017
www.atmos-chem-phys.net/17/2759/2017/
doi:10.5194/acp-17-2759-2017

Atmospheric Chemistry and Physics
Open Access

Widespread and persistent ozone pollution in eastern China during the non-winter season of 2015: observations and source attributions

Guohui Li[1], Naifang Bei[2], Junji Cao[1], Jiarui Wu[1], Xin Long[1], Tian Feng[1,2], Wenting Dai[1], Suixin Liu[1], Qiang Zhang[3], and Xuexi Tie[1]

[1]Key Lab of Aerosol Chemistry and Physics, SKLLQG, Institute of Earth Environment, Chinese Academy of Sciences, Xi'an, China
[2]School of Human Settlements and Civil Engineering, Xi'an Jiaotong University, Xi'an, Shaanxi, China
[3]Department of Earth System Science, Tsinghua University, Beijing, China

Correspondence to: Guohui Li (ligh@ieecas.cn) and Junji Cao (jjcao@ieecas.cn)

Received: 28 September 2016 – Discussion started: 14 October 2016
Revised: 22 January 2017 – Accepted: 25 January 2017 – Published: 23 February 2017

Abstract. Rapid growth of industrialization, transportation, and urbanization has caused increasing emissions of ozone (O_3) precursors recently, enhancing the O_3 formation in eastern China. We show here that eastern China has experienced widespread and persistent O_3 pollution from April to September 2015 based on the O_3 observations in 223 cities. The observed maximum 1 h O_3 concentrations exceed 200 $\mu g\,m^{-3}$ in almost all the cities, 400 $\mu g\,m^{-3}$ in more than 25 % of the cities, and even 800 $\mu g\,m^{-3}$ in six cities in eastern China. The average daily maximum 1 h O_3 concentrations are more than 160 $\mu g\,m^{-3}$ in 45 % of the cities, and the 1 h O_3 concentrations of 200 $\mu g\,m^{-3}$ have been exceeded on over 10 % of days from April to September in 129 cities. Analyses of pollutant observations from 2013 to 2015 have shown that the concentrations of CO, SO_2, NO_2, and $PM_{2.5}$ from April to September in eastern China have considerably decreased, but the O_3 concentrations have increased by 9.9 %. A widespread and severe O_3 pollution episode from 22 to 28 May 2015 in eastern China has been simulated using the Weather Research and Forecasting model coupled to chemistry (WRF-CHEM) to evaluate the O_3 contribution of biogenic and various anthropogenic sources. The model generally performs reasonably well in simulating the temporal variations and spatial distributions of near-surface O_3 concentrations. Using the factor separation approach, sensitivity studies have indicated that the industry source plays the most important role in the O_3 formation and constitutes the culprit of the severe O_3 pollution in eastern China. The transportation source contributes considerably to the O_3 formation, and the O_3 contribution of the residential source is not significant generally. The biogenic source provides a background O_3 source, and also plays an important role in the south of eastern China. Further model studies are needed to comprehensively investigate O_3 formation for supporting the design and implementation of O_3 control strategies, considering rapid changes of emission inventories and photolysis caused by the Atmospheric Pollution Prevention and Control Action Plan released by the Chinese State Council in 2013.

1 Introduction

In the urban planetary boundary layer (PBL), ozone (O_3) is formed as a result of photochemical reactions involving volatile organic compounds (VOCs) and nitrogen oxide (NO_x) in the presence of sunlight (Brasseur et al., 1999):

$$NO_2 + h\upsilon \rightarrow NO + O\left(^3P\right) \quad (290\,nm < \lambda < 420\,nm)$$

$$O\left(^3P\right) + O_2 + M \rightarrow O_3 + M$$

$$O_3 + h\upsilon \rightarrow O_2 + O\left(^1D\right) \quad (290\,nm < \lambda < 329\,nm)$$

$$O\left(^1D\right) + H_2O \rightarrow 2OH$$

$$OH + VOCs + O_2 \rightarrow RO_2 + others$$

$$RO_2 + NO \rightarrow RO + NO_2$$

where $h\upsilon$ represents the energy of a photon; $O(^3P)$ and $O(^1D)$ represent the ground state and electronically excited

oxygen atoms, respectively; RO_2, RO, and OH denote peroxy, oxy-, and hydroxyl radicals, respectively. High O_3 concentrations ([O_3]) are of major environmental concern due to its deleterious impacts on ecosystems (e.g., National Research Council, 1991) and human health (Lippmann, 1993; Weinhold, 2008).

The emissions of O_3 precursors, VOCs and NO_x, have been significantly increased recently in China due to rapid industrialization and urbanization, and increasing transportation activity (e.g., Zhang et al., 2009; Kurokawa et al., 2013; Yang et al., 2015). Satellite measurements have demonstrated that NO_x emissions have been increased by a factor of 2 in central and east China from 2000 to 2006 (Richter et al., 2005). Zhang et al. (2009) have also shown an increasing trend of NO_x emissions with an enhancement of 55 % in China from 2001 to 2006. NO_x emissions have still continued to increase since 2006, due to increasing power plants and vehicles (S. W. Wang et al., 2012; Y. Wang et al., 2013; Yang et al., 2015). In addition, the agriculture has been proposed to have a large potential to produce NO_x (Oikawa et al., 2015). VOC emissions have been estimated to increase by 29 % during 2001–2006 in China (Zhang et al., 2009), and predicted to increase by 49 % by 2020 relative to 2005 levels (Xing et al., 2011). Additionally, modeling studies have been performed to investigate the O_3 pollution in eastern China (Wang et al., 2010; Liu et al., 2012; Situ et al., 2013; Huang et al., 2015). For example, Tie et al. (2013) have analyzed the characteristics of regional O_3 formation to explain the O_3 pollution in Shanghai and its surrounding area using the Weather Research and Forecasting model coupled to chemistry (WRF-CHEM). Using the observation-based chemical model, Xue et al. (2014) have provided insights into the ozone pollution in Beijing, Shanghai, and Guangzhou by analyzing the O_3 precursors and the potential impacts of heterogeneous chemistry.

Increasing O_3 precursor emissions have caused O_3 to be one of the most serious air pollutants of concern during summertime, particularly in eastern China, including the North China Plain (NCP), Yangtze River Delta (YRD), and Pearl River Delta (PRD) (e.g., Xu et al., 2011; Tie et al., 2013; Li et al., 2013; Feng et al., 2016). For example, a maximum O_3 concentration of 286 ppb has been observed in urban plumes from Beijing (Wang et al., 2006). Chen et al. (2015) have reported that the average maximum daily [O_3] exceed 150 $\mu g\,m^{-3}$ in the summer of 2015 at most of monitoring sites in Beijing. Wu et al. (2017) have also shown that, during summertime in 2015 in Beijing, the average O_3 concentration in the afternoon was 163.2 $\mu g\,m^{-3}$, and the frequency of the O_3 exceedance with hourly [O_3] exceeding 200 $\mu g\,m^{-3}$ was 31.8 %. In addition, Cheng et al. (2016) have demonstrated an increasing trend of daily maximum 1 h [O_3] from 2004 to 2015 in Beijing, and Ma et al. (2016) have reported a significant increase of surface O_3 at a rural site in NCP. In the PRD region, the annual average near-surface O_3 level has been reported to increase from 24 ppbv in 2006 to 29 ppbv in 2009, and the maximum 1 h [O_3] can be up to 150–200 ppb in the summer and fall (Ou et al., 2016). Numerous studies have been performed to examine the severe O_3 pollution in China, but were primarily confined to megacities or industrial complexes. Few studies have been conducted for all of eastern China to investigate the O_3 pollution situation and formation.

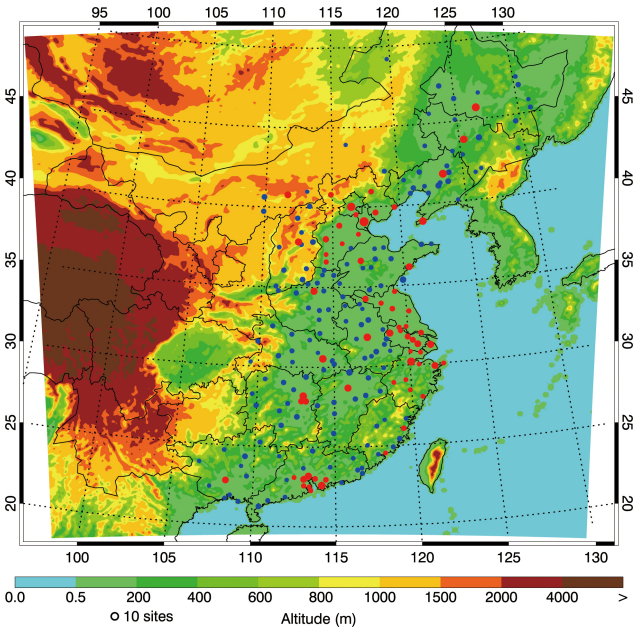

Figure 1. WRF-CHEM simulation domain with topography. The filled circles represent centers of cities with ambient monitoring sites and the size of circles denotes the number of ambient monitoring sites of cities. The red and blue filled circles show the cities with air pollutant observations since 2013 and 2015, respectively.

The China Ministry of Environmental Protection (China MEP) has commenced to release real-time hourly observations of pollutants, including O_3, NO_2, CO, SO_2, $PM_{2.5}$, and PM_{10} (particulate matter with aerodynamic diameter less than 2.5 and 10 µm, respectively) since 2013. In eastern China, there were 65 cities with air pollutant observations in 2013 during summertime, mainly concentrated in Beijing–Tianjin–Hebei (BTH), YRD, and PRD (Fig. 1). In 2015, a total of 223 cities had air pollutant observations in eastern China, providing a good opportunity to explore the O_3 pollution distributions. Therefore, in the present study, the O_3 pollution situation in 2015 is first analyzed from April to September when [O_3] are high in eastern China. A high O_3 episode that occurred in eastern China in 2015 is simulated using the WRF-CHEM model to evaluate the O_3 formation from biogenic and various anthropogenic sources. The WRF-CHEM model configuration and methodology are described in Sect. 2. Data analysis and model results are presented in Sect. 3, and conclusions and discussions are given in Sect. 4.

Table 1. WRF-CHEM model configurations.

Regions	Eastern China
Simulation period	22–28 May 2015
Domain size	350 × 350
Domain center	35° N, 114° E
Horizontal resolution	10 km × 10 km
Vertical resolution	35 vertical levels with a stretched vertical grid with spacing ranging from 30 m near the surface to 500 m at 2.5 and 1 km above 14 km
Microphysics scheme	WSM six-class graupel scheme (Hong and Lim, 2006)
Boundary layer scheme	MYJ TKE scheme (Janjić, 2002)
Surface layer scheme	MYJ surface scheme (Janjić, 2002)
Land-surface scheme	Unified Noah land-surface model (Chen and Dudhia, 2001)
Longwave radiation scheme	Goddard longwave scheme (Chou and Suarez, 2001)
Shortwave radiation scheme	Goddard shortwave scheme (Chou and Suarez, 1999)
Meteorological boundary and initial conditions	NCEP 1° × 1° reanalysis data
Chemical initial and boundary conditions	MOZART 6 h output (Horowitz et al., 2003)
Anthropogenic emission inventory	SAPRC-99 chemical mechanism emissions (Zhang et al., 2009)
Biogenic emission inventory	MEGAN model developed by Guenther et al. (2006)
Model spin-up time	28 h

2 Model and methodology

2.1 WRF-CHEM model and configurations

In the present study, we use a specific version of the WRF-CHEM model (Grell et al., 2005) to investigate the O_3 formation in eastern China. The model is developed by Li et al. (2010, 2011a, b, 2012) at the Molina Center for Energy and the Environment, including a new, flexible gas-phase chemical module and the Models-3 community multiscale air quality (CMAQ) aerosol module developed by the US EPA (Binkowski and Roselle, 2003). The wet deposition of chemical species is calculated using the method in the CMAQ module and the dry deposition parameterization follows Wesely (1989). The fast radiation transfer model (FTUV) is used to calculate photolysis rates (Tie et al., 2003; Li et al., 2005), considering the impacts of aerosols and clouds on the photochemistry (Li et al., 2011b). The ISORROPIA version 1.7 is used to calculate the inorganic aerosols (Nenes et al., 1998). The secondary organic aerosol (SOA) is predicted using a non-traditional SOA module, including the volatility basis set (VBS) modeling approach and SOA contributions from glyoxal and methylglyoxal. Detailed information about the WRF-CHEM model can be found in Li et al. (2010, 2011a, b, 2012).

A high O_3 pollution episode from 22 to 28 May 2015 in eastern China is simulated using the WRF-CHEM model. The WRF-CHEM model adopts one grid with horizontal resolution of 10 km and 35 sigma levels in the vertical direction, and the grid cells used for the domain are 350 × 350 (Fig. 1). The physical parameterizations include the microphysics scheme of Hong and Lim (2006), the Mellor–Yamada–Janjic (MYJ) turbulent kinetic energy (TKE) planetary boundary layer scheme (Janjić, 2002), the unified Noah land-surface model (Chen and Dudhia, 2001), the Goddard longwave (Chou and Suarez, 2001) and shortwave parameterization (Chou and Suarez, 1999). The National Centers for Environmental Prediction (NCEP) 1° × 1° reanalysis data are used to obtain the meteorological initial and boundary conditions, and the meteorological simulations are not nudged in the study. The chemical initial and boundary conditions are interpolated from the 6 h output of MOZART (Horowitz et al., 2003). The spin-up time of the WRF-CHEM model is 28 h, which is generally long enough for simulations considering that the initial and boundary conditions are adopted from MOZART, a global chemical transport model. The SAPRC-99 chemical mechanism is used in the present study. The anthropogenic emissions are developed by Zhang et al. (2009) and Li et al. (2017), including contributions from agriculture, industry, power generation, residential, and transportation sources. The biogenic emissions are calculated online using the MEGAN (Model of Emissions of Gases and Aerosol from Nature) model developed by Guenther et al. (2006). Detailed model configurations are given in Table 1. The simulation domain is shown in Fig. 1.

For discussion convenience, eastern China is divided into four sections: (1) northeast China (including Heilongjiang, Jilin, Liaoning, and the east part of Inner Mongolia, hereafter referred to as NEC), (2) the North China Plain and surrounding areas (including Beijing, Tianjin, Hebei, Shandong, Henan, Shanxi, and the north part of Jiangsu and Anhui, hereafter referred to as NCPs), (3) the YRD and surrounding areas (including the south part of Jiangsu and Anhui, Shanghai, Zhejiang, and Hubei, hereafter referred to as YRDs), and (4) the PRD and surrounding areas (including Fujian, Jiangxi, Hunan, Guangxi, and Guangdong, hereafter referred to as PRDs) (shown in the Supplement, Fig. S1).

Table 2. Observed hourly mass concentrations of pollutants averaged in the afternoon from April to September 2013 and 2015 in 65 cities of eastern China.

Pollutants	CO ($mg\,m^{-3}$)	SO_2 ($\mu g\,m^{-3}$)	NO_2 ($\mu g\,m^{-3}$)	O_3 ($\mu g\,m^{-3}$)	$PM_{2.5}$ ($\mu g\,m^{-3}$)
2013	1.05	24.8	27.7	100.5	46.9
2015	0.77	15.4	23.9	110.5	38.2
Change (%)	−26.7	−37.8	−13.5	+9.9	−18.5

2.2 Statistical methods for comparisons

We use the mean bias (MB) and the index of agreement (IOA) to assess the WRF-CHEM model performance in simulating air pollutants against measurements.

$$\mathrm{MB} = \frac{1}{N}\sum_{i=1}^{N}(P_i - O_i)$$

$$\mathrm{IOA} = 1 - \frac{\sum_{i=1}^{N}(P_i - O_i)^2}{\sum_{i=1}^{N}\left(\left|P_i - \overline{O}\right| + \left|O_i - \overline{O}\right|\right)^2},$$

where P_i and O_i are the calculated and observed pollutant concentrations, respectively. N is the total number of the predictions used for comparisons, and $\overline{O}$ represents the average of the prediction and observation, respectively. The IOA ranges from 0 to 1, with 1 showing perfect agreement of the prediction with the observation.

2.3 Air pollutants measurements

The hourly near-surface CO, NO_2, SO_2, and $PM_{2.5}$ mass concentrations from April to September 2015 in eastern China are released by China MEP and can be downloaded from the website http://www.aqistudy.cn/. China MEP releases the pollutant observations using the mass concentration ($\mu g\,m^{-3}$ or $mg\,m^{-3}$) as the unit. Therefore, in order to keep consistent with the observations, the mass concentration is used in the paper, although the mixing ratio (such as ppbv) is a more common unit used in the literature for air pollutants.

3 Results and discussions

3.1 O_3 pollution in eastern China

Continuous deterioration of air quality in China has engendered the implementation of the Atmospheric Pollution Prevention and Control Action Plan (hereafter referred to as APPCAP), released by Chinese State Council in September 2013 to reduce $PM_{2.5}$ by up to 25 % by 2017 relative to 2012 levels. Therefore, variations of air pollutants from 2013 to 2015 demonstrate the mitigation effects of implementation of the APPCAP on the air quality to a considerable degree. A total of 65 cities, with 427 monitoring sites, have air pollutant observations from 2013 to 2015 during April to September in eastern China (Fig. 1). Considering the occurrence of high [O_3] in the afternoon (12:00–18:00 Beijing time (BJT)), Table 2 provides the average concentrations of air pollutants in the afternoon from April to September in the 65 cites of eastern China in 2013 and 2015. Apparently, implementation of the APPCAP has decreased the mass concentrations of CO, SO_2, NO_2, and $PM_{2.5}$ in eastern China, particularly with regard to SO_2, with a reduction of close to 40 % from 2013 to 2015. The [O_3] however exhibit an increasing trend, enhanced by 9.9 % from 2013 to 2015. Additionally, if the O_3 exceedance is defined as hourly [O_3] exceeding 200 $\mu g\,m^{-3}$ (the second grade of National Ambient Air Quality Standards in China), the O_3 exceedance frequency in the afternoon had increased from 5.2 % in 2013 to 6.8 % in 2015, enhanced by about 31.5 %. The ozone monitoring instrument (OMI) satellite observations have also shown that the annual O_3 concentration has increased by 1.6 % per year over central and eastern China from 2005 to 2014 (Shan et al., 2016).

There are several possible reasons for the O_3 pollution deterioration in eastern China since implementation of the APPCAP. Firstly, if the O_3 production regime in eastern China is VOC sensitive, the decrease of NO_x due to implementation of the APPCAP likely enhances the O_3 formation. Secondly, mitigation of $PM_{2.5}$ or aerosols directly or indirectly increases the photolysis rates and expedites the O_3 formation. Thirdly, increasing transportation activities enhances the emissions of VOCs and semi-VOCs, facilitating the O_3 formation. In addition, variability of meteorological situations also leads to the [O_3] fluctuation (Calkins et al., 2016). Hence, implementation of the APPCAP does not help mitigate [O_3], and unfortunately, severe O_3 pollution has been looming in eastern China.

In 2015, O_3 observations had been performed in 223 cities with 1064 monitoring sites in eastern China, which were used to analyze the O_3 pollution situation from April to September. For comparisons, Fig. 2 shows the distribution of observed maximum 1 h [O_3] in mainland China from April to September in 2015. The cities with the maximum 1 h [O_3] exceeding 300 $\mu g\,m^{-3}$ are mainly concentrated in NCPs, YRDs, and PRD. In eastern China, there are only two cities with the maximum 1 h [O_3] less than 200 $\mu g\,m^{-3}$. About 28 % of cities have observed more than 400 $\mu g\,m^{-3}$ [O_3] (about 200 ppb), showing widespread O_3 pollution in

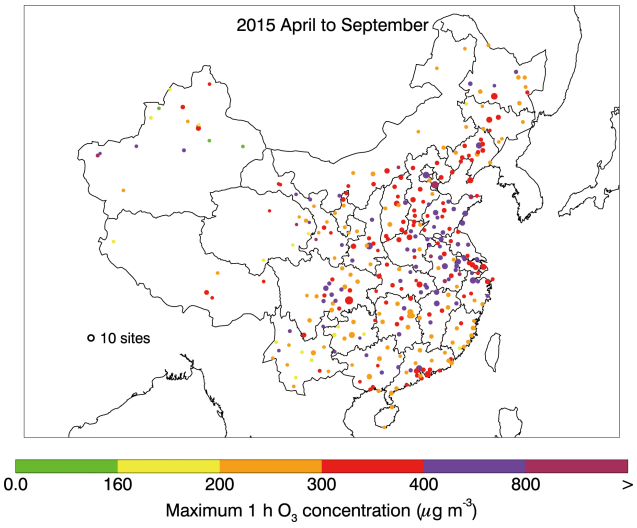

Figure 2. Distribution of observed maximum 1 h [O_3] in mainland China from April to September 2015.

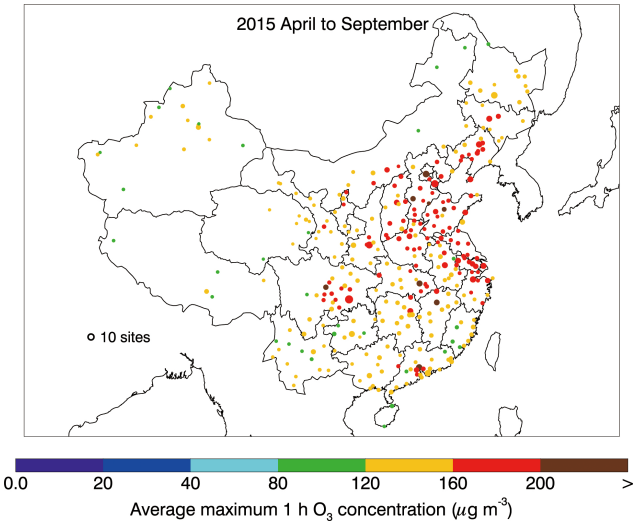

Figure 3. Distribution of average daily maximum 1 h [O_3] in mainland China from April to September 2015.

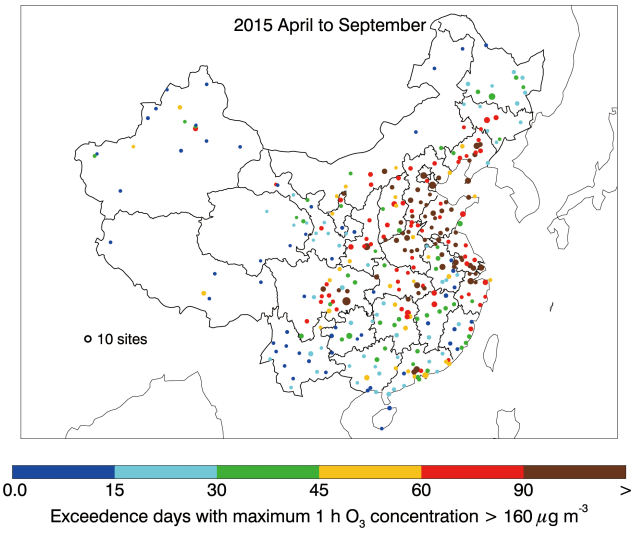

Figure 4. Distribution of days with the maximum 1 h [O_3] exceeding 160 μg m^{-3} in mainland China from April to September 2015.

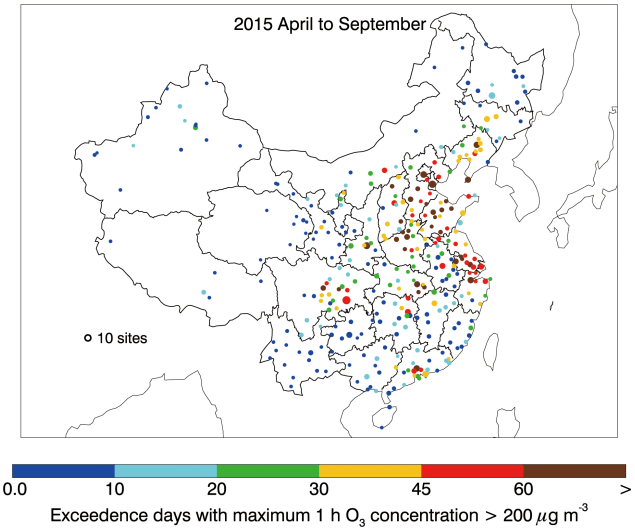

Figure 5. Distribution of days with the maximum 1 h [O_3] exceeding 200 μg m^{-3} in mainland China from April to September 2015.

eastern China. Furthermore, it is worth to note that the observed maximum 1 h [O_3] in six cites exceed 800 μg m^{-3} (about 400 ppb) at a very dangerous level.

Figure 3 presents the distribution of average daily maximum 1 h [O_3] in mainland China from April to September 2015. The average daily maximum 1 h [O_3] are more than 120 μg m^{-3} in more than 95 % of the cities, and 160 μg m^{-3} in 46 % of the cities in eastern China. Particularly, there are seven cities with the average daily maximum 1 h [O_3] exceeding 200 μg m^{-3} during 6 months. Figures 4 and 5 show the distributions of exceedance days with the maximum 1 h [O_3] exceeding 160 and 200 μg m^{-3} in mainland China from April to September 2015, respectively. There are more than 60 days with the maximum 1 h [O_3] exceeding 160 μg m^{-3} in 114 cities, and even more than 90 days in 62 cites in eastern China from April to September. The 1 h [O_3] of 200 μg m^{-3} have been exceeded on over 10 % of days in 129 cities, and on 30 % of days in 38 cities (Fig. 5). Hence, persistent O_3 pollution has occurred in eastern China from April to September in 2015.

Furthermore, in the urban PBL, high [O_3] generally take place under calm or stable circumstances with strong solar radiation. From April to September, the east Asian summer monsoon influences eastern China, causing intensified precipitation which inhibits the high O_3 formation by washing out O_3 precursors and decreasing photolysis rates. Thus, if

excluding rainy days in the analysis, the O_3 pollution becomes more severe in eastern China. For example, in Beijing, there are 54 rainy days and 65 days with the maximum 1 h [O_3] exceeding 200 $\mu g\,m^{-3}$ from May to August in 2015. If it does not rain in Beijing, the occurrence possibility of the maximum 1 h [O_3] exceeding 200 $\mu g\,m^{-3}$ is around 94 %, showing severe and persistent O_3 pollution.

3.2 Model performance

The hourly measurements of O_3 and NO_2 in eastern China are used to validate the WRF-CHEM model simulations. Figure 6 presents the distributions of calculated and observed near-surface [O_3] along with the simulated wind fields at 15:00 BJT from 22 to 27 May 2015. In order to interpret the effect of meteorological and synoptic conditions on the air quality in eastern China, Fig. S2 presents the average geopotential height wind filed at 500 hPa from 22 to 27 May 2015. During the study episode, the NCPs and NEC are generally located behind the trough whose center is located between 120 and 130° E. At the end of May, the main part of subtropical high at 500 hPa was located in the western Pacific, with the ridgeline moving around the 10–15° N. With the onset of the summer monsoon, the subtropical high gradually moves northwards and affects southern China, with more precipitation occurrence over YRDs and PRDs. Figure 6 presents the distributions of calculated and observed near-surface [O_3] along with the simulated wind fields at 15:00 BJT from 22 to 27 May 2015. On 22 May, eastern China is influenced by the high pressure whose center, located over the Yellow Sea, was induced by the high-level trough. The east winds in the south of the high transport humid air into PRDs, causing rainfall weather that substantially decreases [O_3]. The WRF-CHEM model well reproduces the observed low [O_3] in the south of PRDs. In NCPs and YRDs, calm winds, clear sky, and high temperature, induced by the high, facilitate the O_3 formation, and the simulated [O_3] generally exceed 160 $\mu g\,m^{-3}$, which is consistent with the observations. On 23 May, the subtropical high moves northward, also causing the rainfall belt in the south of PRDs to extend northward. The simulated O_3 pollution in NCPs is deteriorated and also extended to NEC, in good agreement with the measurements. From 24 to 25 May, the high pressure located at the Yellow Sea continuously deteriorates the O_3 pollution in eastern China. The simulated and observed O_3 pollution on 25 May is almost widespread in eastern China, and northwest China also experiences high O_3 pollution. On 26 and 27 May, the simulated and observed [O_3] in the north of NCPs and NEC are still high, but in PRDs and YRDs, the [O_3] have been significantly decreased due to the precipitation caused by the subtropical high and summer monsoon.

Generally, the simulated O_3 spatial patterns are consistent with observations, but the model underestimation or overestimation still exists. For example, the model remarkably overestimates the observed [O_3] on 24 May, and also cannot well reproduce the high [O_3] on 25 May in PRD. There are several reasons for the model biases in simulating [O_3] distribution. Firstly, the meteorological situations play a key role in air pollution simulations (Bei et al., 2010, 2012), determining the formation, transformation, diffusion, transport, and removal of the air pollutants. Therefore, uncertainties in meteorological field simulations significantly influence the air pollutant simulations. On 24 May, the model fails to predict the rainy or overcast weather, leading to remarkable overestimation of [O_3] in PRD. Secondly, the 10 km horizontal resolution is used in simulations, which cannot resolve cumulus clouds well. The model overestimates the [O_3] observed in some cities with [O_3] much lower than their surrounding cities, which is primarily caused by the model failure in resolving convections. Thirdly, the fast changes in emissions are not reflected in the emission inventories used in the present study.

Figure 7 provides the diurnal profiles of calculated and observed near-surface [O_3] averaged over the ambient monitoring sites in provinces and municipalities in eastern China during the episode. The model reasonably well reproduces the temporal variations of surface [O_3] compared to observations, e.g., peak [O_3] in the afternoon due to active photochemistry and low [O_3] during nighttime caused by the NO_x titration. Three provinces in NEC (Jilin, Liaoning, and Inner Mongolia) are apparently impacted by the transboundary transport from NCPs when the south winds are prevailing (Fig. 6). Thus, the uncertainties of wind field simulations constitute one of the most important reasons for the model biases in modeling [O_3] in these three provinces. The model underestimates considerably the observed [O_3] in the three provinces (Fig. 7a, c, d), with MBs exceeding 19 $\mu g\,m^{-3}$. The model generally exhibits good performance in simulating [O_3] variations in the provinces of NCPs (Fig. 7e–l) with IOAs exceeding 0.90, but is subject to underestimating the observations, particularly in Beijing which is also significantly influenced by the transboundary transport (Wu et al., 2017). In YRDs, the model cannot well predict the observed [O_3] in Shanghai, which is affected by the sea breeze when the large-scale wind fields are weak. In general, however, current numerical weather prediction models, even in research mode, still have difficulties in producing the location, timing, depth, and intensity of the sea-breeze front (Banta et al., 2005; J. Wang et al., 2013). The model reasonably predicts the [O_3] variations compared to measurements in PRDs (Fig. 7p–t) with IOAs more than 0.7, but overestimates the observed [O_3] with MBs varying from 3.8 to 16.7 $\mu g\,m^{-3}$, showing model biases in modeling precipitation processes.

The comparisons of simulated versus observed distributions and temporal variations of NO_2 mass concentrations ([NO_2]) are shown in the Supplement (Figs. S3 and S4). The simulated high near-surface [NO_2] are mainly concentrated in NCP, YRD, and PRD, which is generally consistent with the measurements. The model also reasonably yields temporal variations of [NO_2] compared to measurements, but the

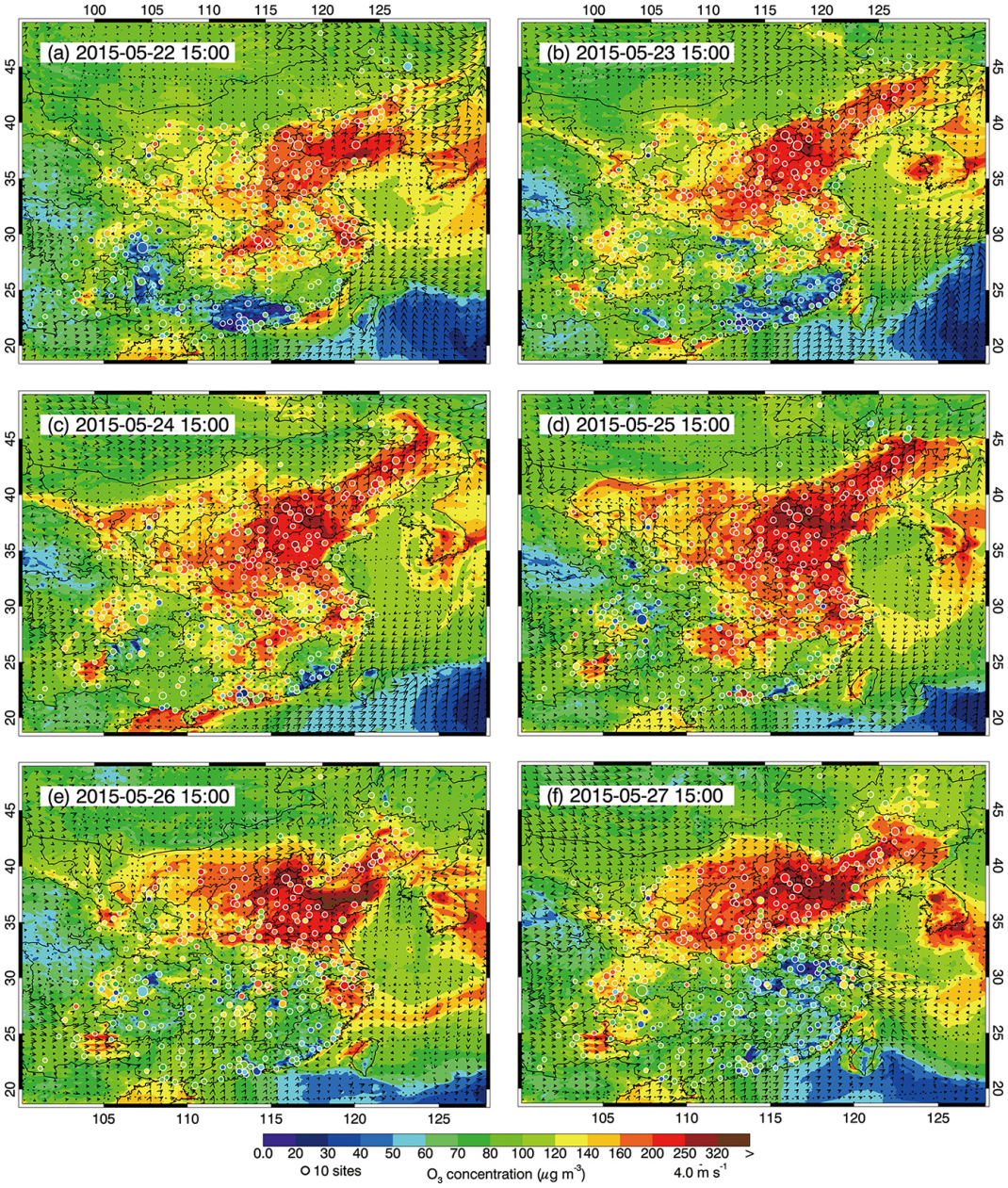

Figure 6. Pattern comparison of simulated versus observed near-surface O_3 at 15:00 BJT from 22 to 27 May 2015. Colored circles: O_3 observations; color contour: O_3 simulations; black arrows: simulated surface winds.

simulations of $[NO_2]$ are not as good as those of $[O_3]$, and the IOAs in Liaoning, Tianjin, and Shanghai are lower than 0.5. The difference between simulations and observations is frequently rather large during nighttime, which is perhaps caused by the model biases in modeling nighttime PBL or the complexity of nighttime chemistry. Another possible reason for NO_x biases in simulations is lack of consideration of the NO_x emissions in the agricultural region, which has been proposed to generate high NO_x emissions under high-temperature conditions (Oikawa et al., 2015). In general, the calculated distributions and variations of $[O_3]$ and $[NO_2]$ are consistent with the corresponding observations, showing that the simulations of meteorological fields and emission inventories are reasonable, providing the base for sensitivity studies.

3.3 Sensitivity studies

O_3 formation in the PBL is a complicated nonlinear process, depending on its precursors of NO_x and VOCs from biogenic and various anthropogenic sources. It is imperative to evaluate the O_3 contribution from various sources for devising

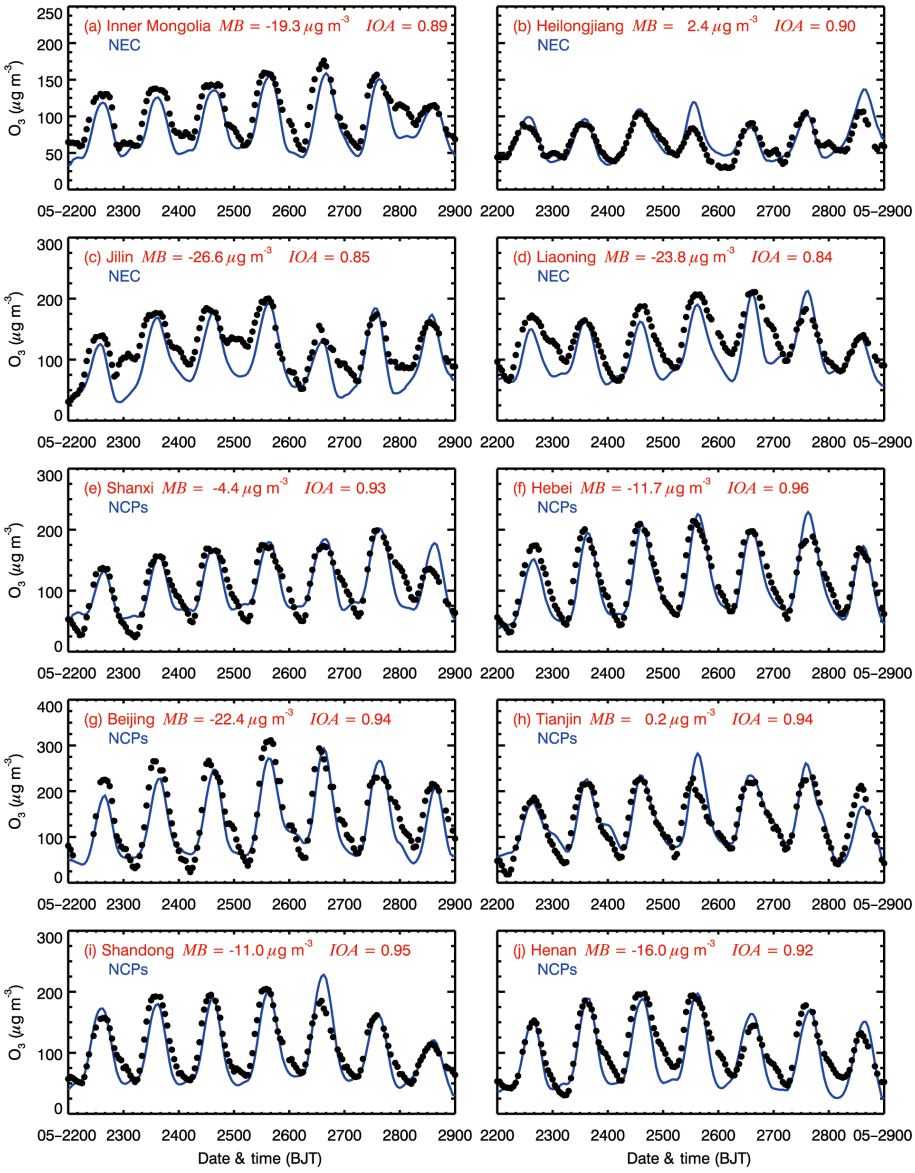

Figure 7.

the O_3 control strategy. Rapid growth of industries, transportation, and urbanization has caused increasing emissions of NO_x and VOCs in eastern China (e.g., Zhang et al., 2009; Huang et al., 2011; Z. Wang et al., 2012; Y. Wang et al., 2013; Yang et al., 2015). Numerous studies have also demonstrated that biogenic VOCs, such as isoprene and monoterpenes, play a considerable role in the O_3 formation in the PBL (e.g., Chameides et al., 1988; Tao et al., 2003; Li et al., 2007, 2014). Therefore, sensitivity studies are used to evaluate the O_3 contributions of biogenic, industry, residential, and transportation sources in eastern China, respectively. It is worth to note that emissions of power plants are directly associated with residential living and industrial activities. Thus, in the study, 75 % of emissions from power plants are assigned to the industry source and the rest are assigned to the residential source according to the ratio of the power consumption used in industrial activities to residential living (Wang et al., 2012).

The factor separation approach (FSA) is used to evaluate the contribution of some emission source to the O_3 concentration by differentiating two model simulations: one with all emission sources and the other without some emission source. Therefore, except the control simulations with all emissions, an additional four sensitivity simulations are performed in which the biogenic, industry, residential, and transportation emissions are excluded, respectively, to assess their corresponding contributions to the O_3 formation in eastern China.

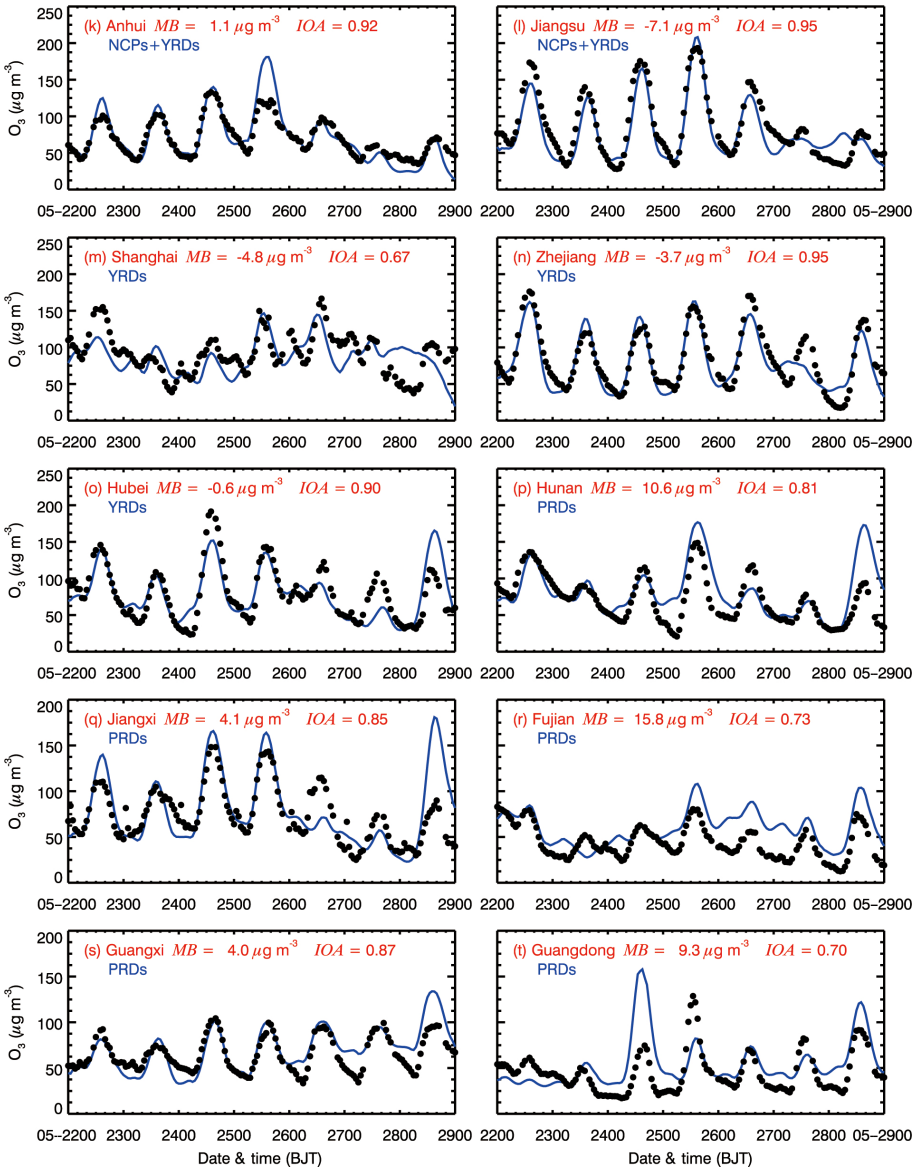

Figure 7. Comparison of measured (black dots) and predicted (blue line) diurnal profiles of near-surface O_3 averaged over all ambient monitoring stations in provinces of eastern China from 22 to 28 May 2015.

Figure 8 shows the contribution of near-surface [O_3] averaged in the afternoon during the whole episode from industry, residential, transportation, and biogenic emissions. The industry source plays a more important role in the O_3 formation than the other three sources, with the O_3 contribution of 10–50 $\mu g\,m^{-3}$ in the afternoon in eastern China. In highly industrialized areas, such as Hebei, Tianjin, Shandong, Zhejiang, etc., the O_3 contribution of the industry source exceeds 30 $\mu g\,m^{-3}$. The residential source is not important in the O_3 formation and contributes about 2–15 $\mu g\,m^{-3}$ O_3 generally. The transportation source plays a considerable role in the O_3 formation, accounting for about 5–30 $\mu g\,m^{-3}$ O_3 in eastern China. The O_3 enhancement due to biogenic emissions is mainly concentrated in NCPs and PRDs, particularly in PRDs, with the O_3 contribution of around 5–50 $\mu g\,m^{-3}$.

In order to further evaluate the contribution of various sources to the [O_3], the hourly near-surface [O_3] in the control simulation are first subdivided into 16 bins with the interval of 20 $\mu g\,m^{-3}$. [O_3] are assembled in the control and sensitivity simulations as the bin [O_3], respectively, and an average of [O_3] in each bin are calculated. Figure 9 shows the contributions of various emission sources to [O_3] in the four sections of eastern China during the episode. The industry emission plays the most important role in the O_3 formation, and is the culprit of the high O_3 pollution. When the [O_3] in the control simulation are less than 100 $\mu g\,m^{-3}$,

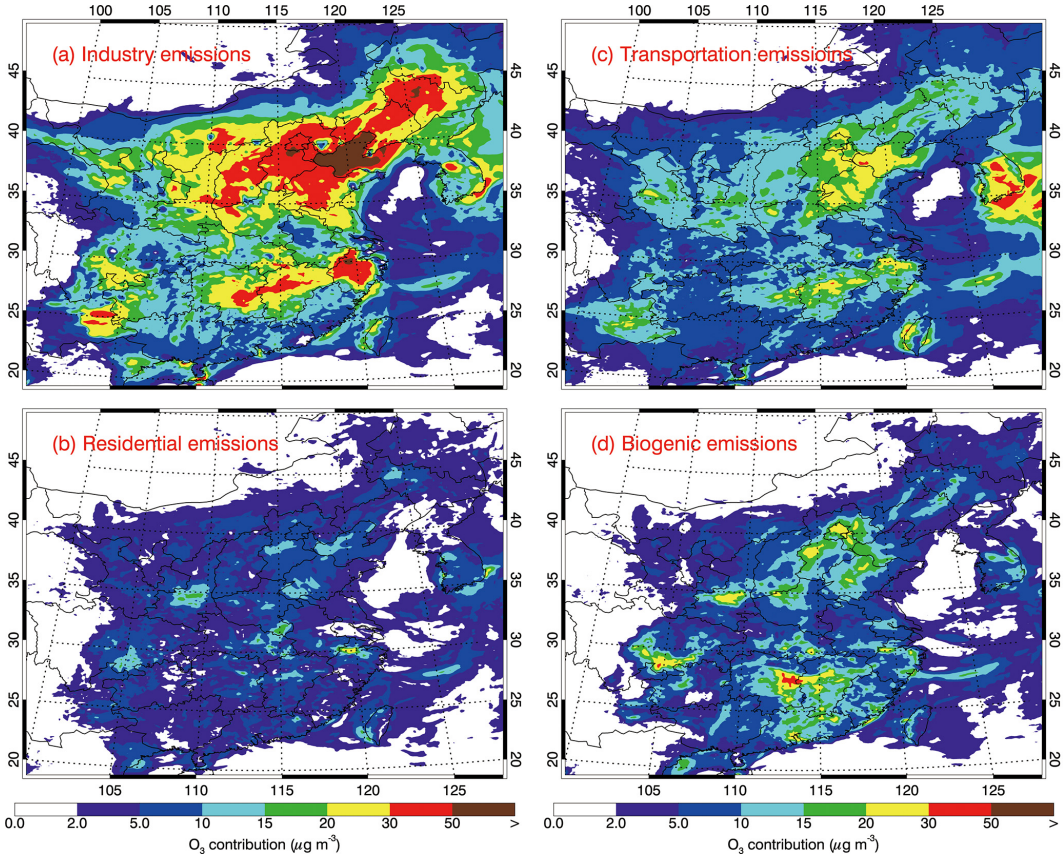

Figure 8. Distributions of the contribution to near-surface [O_3] averaged in the afternoon during the whole episode from **(a)** industry, **(b)** residential, **(c)** transportation, and **(d)** biogenic emissions.

the industry source generally decreases [O_3]. However, when the simulated [O_3] are more than around 200 μg m^{-3}, the O_3 contribution from the industry emissions generally exceeds 50 μg m^{-3}, and when the simulated [O_3] are more than 300 μg m^{-3}, the industrial O_3 contribution can be up to 100 μg m^{-3}, constituting one-third of the [O_3]. The O_3 contribution from the residential source is not significant (generally less than 20 μg m^{-3}). The transportation source plays the second most important role in the O_3 formation in NEC, NCPs, and YRDs, but its O_3 contribution is much less than that from the industry source when the simulated [O_3] are more than 150 μg m^{-3}. VOCs from the biogenic source generally enhance the O_3 formation, providing a background O_3 source. The biogenic source contributes about 10–50 μg m^{-3} O_3 when simulated [O_3] are more than 150 μg m^{-3} in NEC, NCPs, and YRDs. However, in PRDs, the biogenic emissions constitute the second most important O_3 source, with the O_3 contribution exceeding 50 μg m^{-3} when simulated [O_3] are more than 250 μg m^{-3}. Apparently, controlling the industry emissions can substantially mitigate the more severe O_3 pollution in eastern China. If the industry emissions are not considered in model simulations, on average, the [O_3] are generally not more than 200 μg m^{-3} in NEC, YRDs, and PRDs, but still can exceed 160 μg m^{-3}. In addition, excluding the industry source in NCPs does not mitigate [O_3] as remarkably as in the other regions, indicating that other emission sources also play an important role in the O_3 formation. Although the transportation emission is the second most important O_3 source in NEC, NCPs, and PRDs, its O_3 contribution is much less than that from the industry source. Table S1 in the Supplement further presents the emission rates of major O_3 precursors from different emission sources in the model domain during the study episode. The industrial source dominates the VOC and NO_x emissions, playing a key role in the O_3 formation. The transportation source emits more NO_x and active VOCs, such as olefins and aromatics, than the residential source, contributing considerably to the O_3 formation.

Another three sensitivity studies are conducted to further explore the high O_3 formation in eastern China, in which only the industry, residential, and transportation sources are considered, respectively. It is worth to note that biogenic emissions are included in all the three sensitivity simulations considering that the biogenic emissions provide natural O_3 precursors and cannot be anthropogenically controlled. Figure 10 presents the O_3 contributions from individual anthropogenic sources averaged in the afternoon dur-

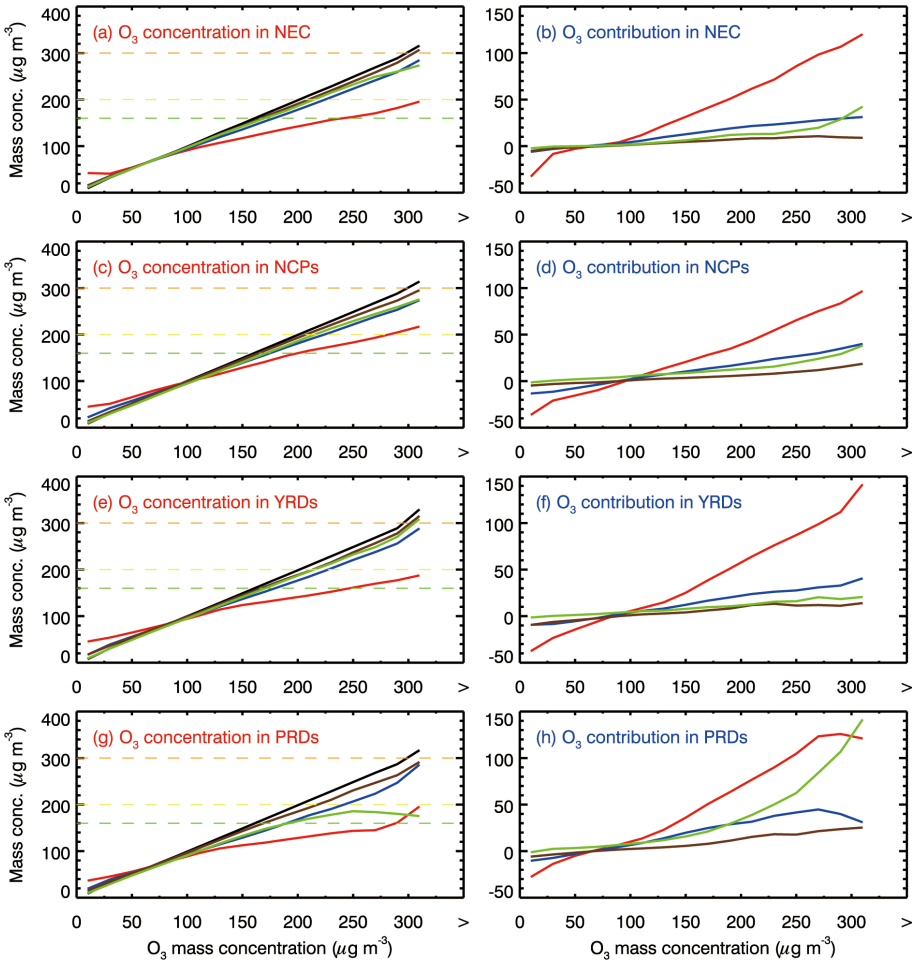

Figure 9. O_3 contributions of industry (red line), residential (brown line), transportation (blue line), and biogenic emissions (green line) in NEC, NCPs, YRDs, and PRDs, as a function of simulated [O_3] in the control case.

ing the whole episode in the four sections of eastern China. If only the industry source is considered or the residential and transportation sources are excluded in the simulation, eastern China still experiences high O_3 pollution. The O_3 contribution of the residential and transportation sources is less than 60 μg m^{-3} on average, further showing the important role of the industry source in the O_3 pollution. When the industry and residential sources are not considered in the simulation, the transportation source still causes the simulated [O_3] to exceed 160 μg m^{-3}, particularly in NCPs. Taking into consideration the very fast increase of vehicles in China recently (X. Wu et al., 2016), the transportation source increasingly constitutes a more important O_3 source, particularly when the industry source is under control. Apparently, when the industry and transportation sources are excluded or only the residential source is included, the high O_3 pollution is significantly mitigated and the simulated [O_3] are less than 160 μg m^{-3} on average. Figure 11 provides the distribution of the [O_3] averaged during the peak time on 25 May when the most serous O_3 pollution occurs during the simulated episode. When only the industry emissions are considered, the O_3 pollution is mitigated considerably in eastern China, but still widespread in NCPs and PRDs. If only considering the transportation source, the O_3 pollution still occurs in NCPs, with the [O_3] exceeding 160 μg m^{-3}. When the industry and transportation sources are excluded, the O_3 pollution is generally under control. Hence, reducing the emissions from industry and transportation is key to mitigating O_3 pollution in eastern China.

4 Summary and conclusions

In the present study, air pollutant observations, released by China MEP, have been analyzed to explore the O_3 pollution situation in eastern China. Analyses of air pollutant observations in 66 cities from 2013 to 2015 have shown that, although implementation of the APPCAP has considerably decreased the CO, SO_2, NO_2, and $PM_{2.5}$ mass concentrations from April to September in eastern China, the [O_3] have in-

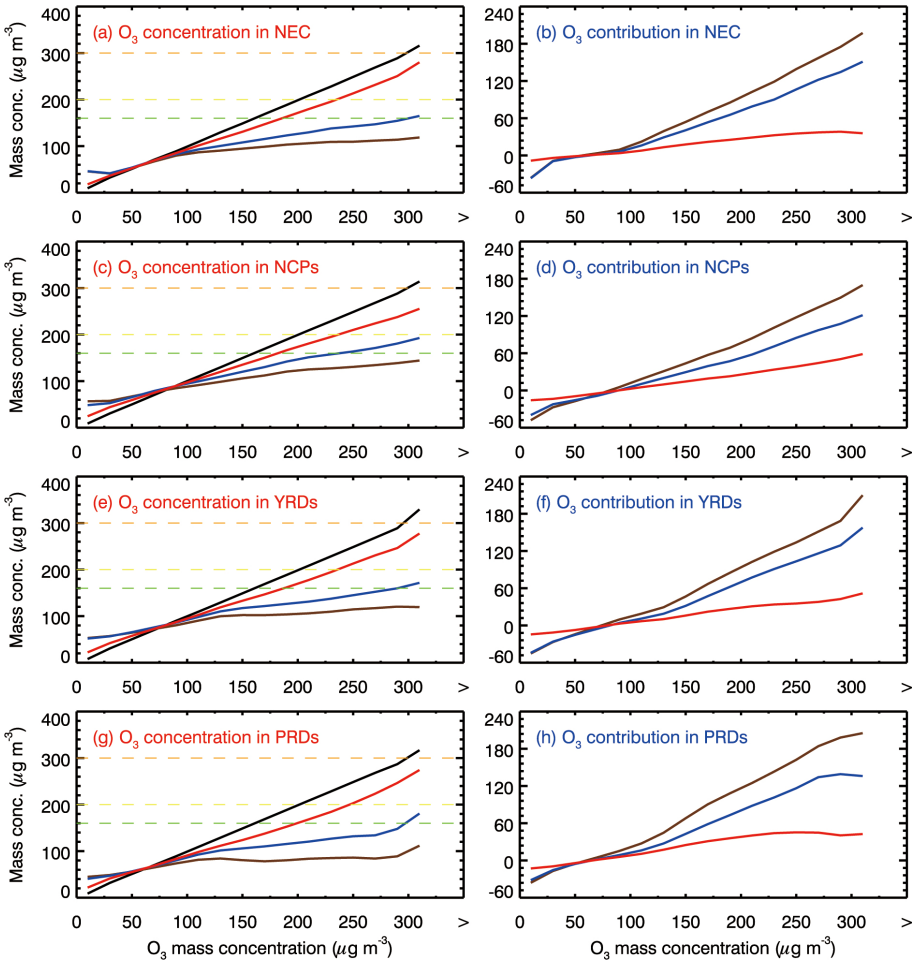

Figure 10. O_3 contributions when only the industry (red line), residential (brown line), and transportation emissions (blue line) are considered in NEC, NCPs, YRDs, and PRDs, as a function of simulated [O_3] in the control case.

creased by 9.2 % and the frequency of O_3 exceedance with hourly [O_3] exceeding 200 μg m^{-3} has increased by about 25 % in the afternoon. Mitigation of NO_x and $PM_{2.5}$ due to implementation of the APPCAP, increasing transportation activities, or variability of meteorological situations perhaps contributes to the deterioration of the O_3 pollution in eastern China.

O_3 observations from April to September in 2015 have shown that eastern China has experienced widespread and persistent O_3 pollution. Only two cities in eastern China have observed the maximum 1 h [O_3] of less than 200 μg m^{-3}. Over 25 % of cities have observed the maximum 1 h [O_3] exceeding 400 μg m^{-3}; particularly, more than 800 μg m^{-3} [O_3] have been observed in six cities in eastern China. The average daily maximum 1 h [O_3] from April to September exceed 160 μg m^{-3} in 45 % of cities in eastern China, and the 1 h [O_3] of 200 μg m^{-3} have been exceeded on over 10 % of days from April to September in 129 cities, and on 40 % of days in 10 cities.

A widespread and severe O_3 pollution episode from 22 to 28 May 2015 in eastern China has been simulated using the WRF-CHEM model. The model generally simulates reasonably well the temporal variations and spatial distributions of near-surface [O_3], but the uncertainties of meteorological fields or emission inventories still cause model overestimation or underestimation. The model performs reasonably in simulating NO_2, but the model biases are rather large during nighttime.

FSA is utilized to assess the O_3 contribution of biogenic and various anthropogenic sources. Sensitivity studies have shown that the industry source plays the most important role in the O_3 pollution formation. When the simulated [O_3] are more than around 200 μg m^{-3}, the O_3 contribution from the industry emissions generally exceeds 50 μg m^{-3} in eastern China, particularly when the simulated [O_3] exceed 300 μg m^{-3}, the industrial O_3 contribution constitutes one-third of the [O_3]. The transportation emission is the second most important O_3 source in NEC, YRDs, and PRDs, but its O_3 contribution is much less than that from the indus-

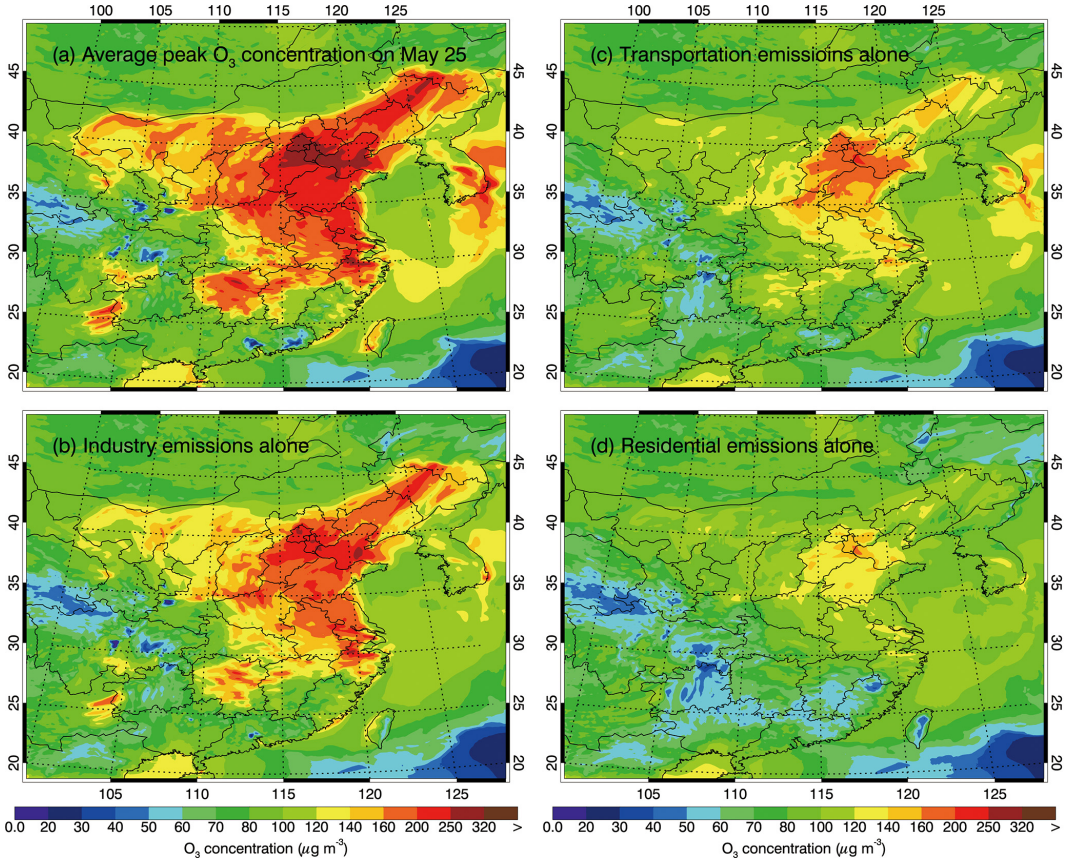

Figure 11. Distributions of the average O_3 concentration during peak time with **(a)** all anthropogenic emissions, **(b)** industry emissions alone, **(c)** residential emissions alone, and **(d)** transportation emissions alone on May 2015.

try source when the simulated [O_3] exceed 150 $\mu g\,m^{-3}$. The biogenic source plays a more important role in O_3 formation than the transportation source in PRDs, with the O_3 contribution exceeding 50 $\mu g\,m^{-3}$ when simulated [O_3] are more than 250 $\mu g\,m^{-3}$. In general, the O_3 contribution from the residential source is not significant. Further sensitivity studies have also indicated that if only considering the residential source or excluding the industry and transportation sources in simulations, the O_3 pollution in eastern China could be significantly improved. Only the industry or transportation sources still cause O_3 pollution, particularly with regard to the industry source.

Widespread and persistent O_3 pollution poses adverse impacts on ecosystems and human health. Considering the key role of the industry source in the high O_3 formation, mitigation of the industry source becomes the top choice to improve the O_3 pollution in eastern China, particularly with regard to the VOC emissions that are still not fully considered in the current air pollutant control strategy. Rapid increase of vehicles also enhances the VOC and NO_x emissions and the transportation source plays an increasingly important role in the O_3 pollution. In addition, the rapid decrease of $PM_{2.5}$ due to implementation of the APPCAP reduces the aerosol and cloud optical depth, which is subject to enhance the O_3 formation by increasing the photolysis. Hence, stringent control strategies of VOCs and NO_x need to be designed comprehensively and implemented to avoid the looming severe O_3 pollution in eastern China.

Although the model performs generally well in simulating O_3 and NO_2 during a 7-day O_3 pollution episode in eastern China, uncertainties from meteorological field simulations and emission inventory still cause model biases. Meteorological conditions play a key role in the formation of air pollution, determining the formation, transformation, diffusion, transport, and removal of the air pollutants in the atmosphere (Bei et al., 2010, 2012). A nudging of wind and temperature fields using observations generally improves the simulation of meteorological fields, reducing the model biases in reproducing the O_3 temporal variation and spatial distribution. Thus, future studies are needed to improve the meteorological fields using the data assimilation, such as the four-dimension data assimilation (FDDA). Taking into consideration the complexity of the O_3 formation and rapid changes of emission inventories, further model studies need to be performed to investigate the O_3 formation for supporting the

design and implementation of emission control strategies, based on the improved meteorological field simulations.

5 Data availability

The real-time O_3 and $PM_{2.5}$ data are accessible to the public at http://106.37.208.233:20035/ (MEP China, 2013a). One can also access the historic profile of observed ambient pollutants through visiting http://www.aqistudy.cn/ (MEP China, 2013b).

The Supplement related to this article is available online at doi:10.5194/acp-17-2759-2017-supplement.

Competing interests. The authors declare that they have no conflict of interest.

Acknowledgements. This work was supported by the National Natural Science Foundation of China (no. 41275153) and by the "Strategic Priority Research Program" of the Chinese Academy of Sciences, grant no. XDB05060500. Guohui Li is also supported by the "Hundred Talents Program" of the Chinese Academy of Sciences. Naifang Bei is supported by the National Natural Science Foundation of China (no. 41275101). Wenting Dai is supported by the National Natural Science Foundation of China (no. 41503117).

Edited by: L. Molina
Reviewed by: two anonymous referees

References

Banta, R. M., Senff, C. J., Nielsen-Gammon, J., Darby, L. S., Ryerson, T. B., Alvarez, R. J., Sandberg, S. R., Williams, E. J., and Trainer, M.: A bad air day in Houston, B. Am. Meteorol. Soc., 86, 657–669, doi:10.1175/bams-86-5-657, 2005.

Bei, N., Lei, W., Zavala, M., and Molina, L. T.: Ozone predictabilities due to meteorological uncertainties in the Mexico City basin using ensemble forecasts, Atmos. Chem. Phys., 10, 6295–6309, doi:10.5194/acp-10-6295-2010, 2010.

Bei, N., Li, G., and Molina, L. T.: Uncertainties in SOA simulations due to meteorological uncertainties in Mexico City during MILAGRO-2006 field campaign, Atmos. Chem. Phys., 12, 11295–11308, doi:10.5194/acp-12-11295-2012, 2012.

Binkowski, F. S. and Roselle, S. J.: Models-3 community multiscale air quality (CMAQ) model aerosol component – 1. Model description, J. Geophys. Res., 108, 4183, doi:10.1029/2001jd001409, 2003.

Brasseur, G. P., Orlando, J. J., and Tyndall, G. S.: Atmospheric chemistry and global change, Oxford University Press, Cambridge, USA, 654 pp., 1999.

Calkins, C., Ge, C., Wang, J., Anderson, M., and Yang, K.: Effects of meteorological conditions on sulfur dioxide air pollution in the North China Plain during winters of 2006–2015, Atmos. Environ., 147, 296–309, 2016.

Chameides, W. L., Lindsay, R. W., Richardson, J., and Kiang, C. S.: The role of biogenic hydrocarbons in urban photochemical smog – Atlanta as a case-study, Science, 241, 1473–1475, doi:10.1126/science.3420404, 1988.

Chen, F. and Dudhia, J.: Coupling an advanced land surface-hydrology model with the Penn State-NCAR MM5 modeling system, Part I: Model implementation and sensitivity, Mon. Weather Rev., 129, 569–585, doi:10.1175/1520-0493(2001)129<0569:caalsh>2.0.co;2, 2001.

Chen, W., Yan, L., and Zhao, H. M.: Seasonal Variations of Atmospheric Pollution and Air Quality in Beijing, Atmosphere, 6, 1753–1770, doi:10.3390/atmos6111753, 2015.

Cheng, N., Li, Y., Zhang, D., Chen, T., Sun, F., Chen, C., and Meng, F.: Characteristics of Ground Ozone Concentration over Beijing from 2004 to 2015: Trends, Transport, and Effects of Reductions, Atmos. Chem. Phys. Discuss., doi:10.5194/acp-2016-508, in review, 2016.

Chou, M.-D. and Suarez, M. J.: A solar radiation parameterization for atmospheric studies, NASA Tech. Rep. NASA/TM-1999-10460, 15, 38 pp., 1999.

Chou, M.-D. and Suarez, M. J.: A thermal infrared radiation parameterization for atmospheric studies, NASA/TM-2001-104606, 19, 55 pp., 2001.

Feng, T., Bei, N., Huang, R.-J., Cao, J., Zhang, Q., Zhou, W., Tie, X., Liu, S., Zhang, T., Su, X., Lei, W., Molina, L. T., and Li, G.: Summertime ozone formation in Xi'an and surrounding areas, China, Atmos. Chem. Phys., 16, 4323–4342, doi:10.5194/acp-16-4323-2016, 2016.

Grell, G. A., Peckham, S. E., Schmitz, R., McKeen, S. A., Frost, G., Skamarock, W. C., and Eder, B.: Fully coupled "online" chemistry within the WRF model, Atmos. Environ., 39, 6957–6975, doi:10.1016/j.atmosenv.2005.04.027, 2005.

Guenther, A., Karl, T., Harley, P., Wiedinmyer, C., Palmer, P. I., and Geron, C.: Estimates of global terrestrial isoprene emissions using MEGAN (Model of Emissions of Gases and Aerosols from Nature), Atmos. Chem. Phys., 6, 3181–3210, doi:10.5194/acp-6-3181-2006, 2006.

Huang, M., Carmichael, G. R., Spak, S. N., Adhikary, B., Kulkarni, S., Cheng, Y., Wei, C., Tang, Y., D'Allura, A., Wennberg, P. O., Huey, G. L., Dibb, J. E., Jimenez, J. L., Cubison, M. J., Weinheimer, A. J., Kaduwela, A., Cai, C., Wong, M., Bradley Pierce, R., Al-Saadi, J. A., Streets, D. G., and Zhang, Q.: Multi-scale modeling study of the source contributions to near-surface ozone and sulfur oxides levels over California during the ARCTAS-CARB period, Atmos. Chem. Phys., 11, 3173–3194, doi:10.5194/acp-11-3173-2011, 2011.

Huang, J., Liu, H., Crawford, J. H., Chan, C., Considine, D. B., Zhang, Y., Zheng, X., Zhao, C., Thouret, V., Oltmans, S. J., Liu, S. C., Jones, D. B. A., Steenrod, S. D., and Damon, M. R.: Origin of springtime ozone enhancements in the lower troposphere over Beijing: in situ measurements and model analysis, Atmos. Chem. Phys., 15, 5161–5179, doi:10.5194/acp-15-5161-2015, 2015.

Hong, S.-Y. and Lim, J.-O. J.: The WRF Single-Moment 6-Class Microphysics Scheme (WSM6), Asia-Pac. J. Atmos. Sci., 42, 129–151, 2006.

Horowitz, L. W., Walters, S., Mauzerall, D. L., Emmons, L. K., Rasch, P. J., Granier, C., Tie, X. X., Lamarque, J. F., Schultz, M. G., Tyndall, G. S., Orlando, J. J., and Brasseur, G. P.: A global simulation of tropospheric ozone and related tracers: Description and evaluation of MOZART, version 2, J. Geophys. Res., 108, 4784, doi:10.1029/2002jd002853, 2003.

Janjić, Z. I.: Nonsingular Implementation of the Mellor–Yamada Level 2.5 Scheme in the NCEP Meso Model, Ncep Office Note, 436 pp., 2002.

Kurokawa, J., Ohara, T., Morikawa, T., Hanayama, S., Janssens-Maenhout, G., Fukui, T., Kawashima, K., and Akimoto, H.: Emissions of air pollutants and greenhouse gases over Asian regions during 2000–2008: Regional Emission inventory in ASia (REAS) version 2, Atmos. Chem. Phys., 13, 11019–11058, doi:10.5194/acp-13-11019-2013, 2013.

Li, G., Zhang, R., Fan, J., and Tie, X.: Impacts of black carbon aerosol on photolysis and ozone, J. Geophys. Res., 110, D23206, doi:10.1029/2005jd005898, 2005.

Li, G., Zhang, R., Fan, J., and Tie, X.: Impacts of biogenic emissions on photochemical ozone production in Houston, Texas, J. Geophys. Res., 112, D10309, doi:10.1029/2006jd007924, 2007.

Li, G., Lei, W., Zavala, M., Volkamer, R., Dusanter, S., Stevens, P., and Molina, L. T.: Impacts of HONO sources on the photochemistry in Mexico City during the MCMA-2006/MILAGO Campaign, Atmos. Chem. Phys., 10, 6551–6567, doi:10.5194/acp-10-6551-2010, 2010.

Li, G., Bei, N., Tie, X., and Molina, L. T.: Aerosol effects on the photochemistry in Mexico City during MCMA-2006/MILAGRO campaign, Atmos. Chem. Phys., 11, 5169–5182, doi:10.5194/acp-11-5169-2011, 2011a.

Li, G., Zavala, M., Lei, W., Tsimpidi, A. P., Karydis, V. A., Pandis, S. N., Canagaratna, M. R., and Molina, L. T.: Simulations of organic aerosol concentrations in Mexico City using the WRF-CHEM model during the MCMA-2006/MILAGRO campaign, Atmos. Chem. Phys., 11, 3789–3809, doi:10.5194/acp-11-3789-2011, 2011b.

Li, G., Lei, W., Bei, N., and Molina, L. T.: Contribution of garbage burning to chloride and PM2.5 in Mexico City, Atmos. Chem. Phys., 12, 8751–8761, doi:10.5194/acp-12-8751-2012, 2012.

Li, G., Bei, N. F., Zavala, M., and Molina, L. T.: Ozone formation along the California Mexican border region during Cal-Mex 2010 field campaign, Atmos. Environ., 88, 370–389, doi:10.1016/j.atmosenv.2013.11.067, 2014.

Li, M., Zhang, Q., Kurokawa, J.-I., Woo, J.-H., He, K., Lu, Z., Ohara, T., Song, Y., Streets, D. G., Carmichael, G. R., Cheng, Y., Hong, C., Huo, H., Jiang, X., Kang, S., Liu, F., Su, H., and Zheng, B.: MIX: a mosaic Asian anthropogenic emission inventory under the international collaboration framework of the MICS-Asia and HTAP, Atmos. Chem. Phys., 17, 935–963, doi:10.5194/acp-17-935-2017, 2017.

Li, Y., Lau, A. K. H., Fung, J. C. H., Zheng, J. Y., and Liu, S. C.: Importance of NO_x control for peak ozone reduction in the Pearl River Delta region, J. Geophys. Res.-Atmos., 118, 9428–9443, doi:10.1002/jgrd.50659, 2013.

Lippmann, M.: Health-effects of tropospheric ozone – review of recent research findings and their implications to ambient air-quality standards, J. Expo. Anal. Environ. Epidemiol., 3, 103–129, 1993.

Liu, Z., Wang, Y., Gu, D., Zhao, C., Huey, L. G., Stickel, R., Liao, J., Shao, M., Zhu, T., Zeng, L., Amoroso, A., Costabile, F., Chang, C.-C., and Liu, S.-C.: Summertime photochemistry during CAREBeijing-2007: ROx budgets and O_3 formation, Atmos. Chem. Phys., 12, 7737–7752, doi:10.5194/acp-12-7737-2012, 2012.

Ma, Z., Xu, J., Quan, W., Zhang, Z., Lin, W., and Xu, X.: Significant increase of surface ozone at a rural site, north of eastern China, Atmos. Chem. Phys., 16, 3969–3977, doi:10.5194/acp-16-3969-2016, 2016.

Ministry of Environmental Protection, China (MEP China): Air Quality Observation Real-time Release Platform of MEP Data Center, available at: http://106.37.208.233:20035/, 2013a.

Ministry of Environmental Protection, China (MEP China): Online Monitoring and Analysis Platform of China Air Quality, available at: http://www.aqistudy.cn/, 2013b.

National Research Council: Rethinking the Ozone Problem in Urban and Regional Air Pollution, National Academy Press, Washington, DC, 1991.

Nenes, A., Pandis, S. N., and Pilinis, C.: ISORROPIA: A new thermodynamic equilibrium model for multiphase multicomponent inorganic aerosols, Aquat. Geochem., 4, 123–152, doi:10.1023/a:1009604003981, 1998.

Oikawa, P. Y., Ge, C., Wang, J., Eberwein, J. R., Liang, L. L., Allsman, L. A., Grantz, D. A., and Jenerette, G. D.: 2015. Unusually high soil nitrogen oxide emissions influence air quality in a high-temperature agricultural region, Nat. Commun., 6, 8753–8757, 2015.

Ou, J. M., Yuan, Z. B., Zheng, J. Y., Huang, Z. J., Shao, M., Li, Z. K., Huang, X. B., Guo, H., and Louie, P. K. K.: Ambient Ozone Control in a Photochemically Active Region: Short Term Despiking or Long-Term Attainment?, Environ. Sci. Technol., 50, 5720–5728, doi:10.1021/acs.est.6b00345, 2016.

Richter, A., Burrows, J. P., Nuss, H., Granier, C., and Niemeier, U.: Increase in tropospheric nitrogen dioxide over China observed from space, Nature, 437, 129–132, doi:10.1038/nature04092, 2005.

Shan, Y., Li, L., Liu, Q., Chen, Y., Shi, Y., Liu, X., and Qiao, L.: Spatial-Temporal Distribution of ozone and its precursors over central and eastern China based on OMI Data, Res. Environ. Sci., 29, 1128–1136, 2016.

Situ, S., Guenther, A., Wang, X., Jiang, X., Turnipseed, A., Wu, Z., Bai, J., and Wang, X.: Impacts of seasonal and regional variability in biogenic VOC emissions on surface ozone in the Pearl River delta region, China, Atmos. Chem. Phys., 13, 11803–11817, doi:10.5194/acp-13-11803-2013, 2013.

Tao, Z. N., Larson, S. M., Wuebbles, D. J., Williams, A., and Caughey, M.: A summer simulation of biogenic contributions to ground-level ozone over the continental United States, J. Geophys. Res., 108, 4404, doi:10.1029/2002jd002945, 2003.

Tie, X., Madronich, S., Walters, S., Zhang, R. Y., Rasch, P., and Collins, W.: Effect of clouds on photolysis and oxidants in the troposphere, J. Geophys. Res., 108, 4642, doi:10.1029/2003jd003659, 2003.

Tie, X., Geng, F., Guenther, A., Cao, J., Greenberg, J., Zhang, R., Apel, E., Li, G., Weinheimer, A., Chen, J., and Cai, C.: Megacity impacts on regional ozone formation: observations and WRF-Chem modeling for the MIRAGE-Shanghai field campaign, At-

mos. Chem. Phys., 13, 5655–5669, doi:10.5194/acp-13-5655-2013, 2013.

Wang, J., Ge, C., Yang, Z., Hyer, E. J., Reid, J. S., Chew, B.-N., Mahmud, M., Zhang, Y., and Zhang, M.: Mesoscale modeling of smoke transport over the Southeast Asian Maritime Continent: interplay of sea breeze, trade wind, typhoon, and topography, Atmos. Res., 122, 486–503, 2013.

Wang, S. W., Zhang, Q., Streets, D. G., He, K. B., Martin, R. V., Lamsal, L. N., Chen, D., Lei, Y., and Lu, Z.: Growth in NO_x emissions from power plants in China: bottom-up estimates and satellite observations, Atmos. Chem. Phys., 12, 4429–4447, doi:10.5194/acp-12-4429-2012, 2012.

Wang, T., Ding, A. J., Gao, J., and Wu, W. S.: Strong ozone production in urban plumes from Beijing, China, Geophys. Res. Lett., 33, L21806, doi:10.1029/2006gl027689, 2006.

Wang, X., Zhang, Y., Hu, Y., Zhou, W., Lu, K., Zhong, L., Zeng, L., Shao, M., Hu, M., and Russell, A. G.: Process analysis and sensitivity study of regional ozone formation over the Pearl River Delta, China, during the PRIDE-PRD2004 campaign using the Community Multiscale Air Quality modeling system, Atmos. Chem. Phys., 10, 4423–4437, doi:10.5194/acp-10-4423-2010, 2010.

Wang, Y., Zhang, Q. Q., He, K., Zhang, Q., and Chai, L.: Sulfate-nitrate-ammonium aerosols over China: response to 2000–2015 emission changes of sulfur dioxide, nitrogen oxides, and ammonia, Atmos. Chem. Phys., 13, 2635–2652, doi:10.5194/acp-13-2635-2013, 2013.

Wang, Z., Zeng, H., Wei, Y., and Zhang, Y.: Regional total factor energy efficiency: An empirialcal analysis of inudstrial sectior in China, Appl. Energ., 2012, 115–123, 2012.

Weinhold, B.: Ozone nation – EPA standard panned by the people, Environ. Health Persp., 116, 302–305, 2008.

Wesely, M. L.: Parameterization of surface resistances to gaseous dry deposition in regional-scale numerical models, Atmos. Environ., 23, 1293–1304, doi:10.1016/0004-6981(89)90153-4, 1989.

Wu, J., Li, G., Cao, J., Bei, N., Wang, Y., Feng, T., Huang, R., Liu, S., Zhang, Q., and Tie, X.: Contributions of trans-boundary transport to summertime air quality in Beijing, China, Atmos. Chem. Phys., 17, 2035–2051, doi:10.5194/acp-17-2035-2017, 2017

Wu, X., Wu, Y., Zhang, S., Liu, H., Fu, L., and Hao, J.: Assessment of vehicle emission programs in China during 1998–2013: Achievement, challlenges and implications, Environ. Pollut., 214, 556–567, 2016.

Xing, J., Wang, S. X., Chatani, S., Zhang, C. Y., Wei, W., Hao, J. M., Klimont, Z., Cofala, J., and Amann, M.: Projections of air pollutant emissions and its impacts on regional air quality in China in 2020, Atmos. Chem. Phys., 11, 3119–3136, doi:10.5194/acp-11-3119-2011, 2011.

Xu, J., Ma, J. Z., Zhang, X. L., Xu, X. B., Xu, X. F., Lin, W. L., Wang, Y., Meng, W., and Ma, Z. Q.: Measurements of ozone and its precursors in Beijing during summertime: impact of urban plumes on ozone pollution in downwind rural areas, Atmos. Chem. Phys., 11, 12241–12252, doi:10.5194/acp-11-12241-2011, 2011.

Xue, L. K., Wang, T., Gao, J., Ding, A. J., Zhou, X. H., Blake, D. R., Wang, X. F., Saunders, S. M., Fan, S. J., Zuo, H. C., Zhang, Q. Z., and Wang, W. X.: Ground-level ozone in four Chinese cities: precursors, regional transport and heterogeneous processes, Atmos. Chem. Phys., 14, 13175–13188, doi:10.5194/acp-14-13175-2014, 2014.

Yang, X. F., Liu, H., Man, H. Y., and He, K. B.: Characterization of road freight transportation and its impact on the national emission inventory in China, Atmos. Chem. Phys., 15, 2105–2118, doi:10.5194/acp-15-2105-2015, 2015.

Zhang, Q., Streets, D. G., Carmichael, G. R., He, K. B., Huo, H., Kannari, A., Klimont, Z., Park, I. S., Reddy, S., Fu, J. S., Chen, D., Duan, L., Lei, Y., Wang, L. T., and Yao, Z. L.: Asian emissions in 2006 for the NASA INTEX-B mission, Atmos. Chem. Phys., 9, 5131–5153, doi:10.5194/acp-9-5131-2009, 2009.